J. Microbiol. Biotechnol. (2008), **18**(5), 889–896

JOURNAL OF MICROBIOLOGY AND BIOTECHNOLOGY

Modeling of Esterase Production from *Saccharomyces cerevisiae*

Thilakavathi[1], Tanmay Basak[2], and Tapobrata Panda[1]*

[1]*Biochemical Engineering Laboratory (MSB140A 8MS B235A), Chennai6002, India*
[2]*Department of Chemical Engineering, Indian Institute of Technology Madras, Chennai 600036, India*

Received: July 4, 2007 / Accepted: October 17, 2007

A suitable simple model tested by experiments is required to address complex biological reactions like esterase synthesis by *Saccharomyces cerevisiae*. Such an approach might be the answer to a proper bioprocessing strategy. In this regard, a logistic model for esterase production from *Saccharomyces cerevisiae* has been developed, which predicts well the cell mass, the carbon source (glucose) consumption, and the esterase activity. The accuracy of the model has been statistically examined by using the Student's *t*-test. The parameter sensitivity analysis showed that all five parameters (μ_m, K_s, X_m, $Y_{x/s}$, and $Y_{p/x}$) have significant influence on the predicted values of esterase activity.

Keywords: Esterase, logistic model, parameter sensitivity, *Saccharomyces cerevisiae*

Esterase splits esters into an acid and an alcohol in a chemical reaction with water during hydrolysis. Wide ranges of different esterases exist that differ in substrate specificity, protein structure, and biological function [13, 18, 20]. Esterase is an important biocatalyst for the industrial production of chiral intermediates. In general, esterases are easy to handle. The enzymes are quite stable, which is important for industrial processes. Enzymes, particularly esterases and lipases, are recognized as functional catalysts for asymmetric synthesis, and in several situations, their stereochemical control cannot be equaled by nonenzymatic catalysis [26]. Additionally, esterase is characterized by a large range of substrate selectivity combined with high stereoselectivity. In contrast to lipases, esterases are more specific to short-chain fatty acids and are used in aqueous or two-phase systems. Esterases are also used for the optical resolution of racemic mixtures. There are a few esterases that also hydrolyze tertiary alcohols. These enzymes have also been used to separate endo-/exo-mixtures and for the regioselective hydrolysis of an ester group in the presence of a second ester function. Specific types of esterases are found useful in the paper and pulp beer manufacturing, perfumes, and pharmaceuticals industries. Specifically, esterases from *Saccharomyces cerevisiae* are involved in the development of flavor for food and alcoholic beverages like sake, beer, and wine. The main advantages of microbial esterases are high selectivity and activity, animal-free material, broad applicability, and excellent catalytic performance [9, 12, 23].

In order to produce a large quantity of esterases, one needs to propose a suitable process strategy based on a quantitative concept. In this context, a suitable and reliable kinetic model is necessary. The reason to develop an unstructured model for esterase production is its simplicity. This kinetic model is a useful tool for the study and control of industrial microbial processes. Kinetic studies based on unstructured models for products from various microorganisms are available in earlier works [3, 4, 8, 10, 11, 21, 24, 29]. The literature shows that the equations of the unstructured model differ with the product synthesized and also the microorganism used. This implies that the same set of model equations that is applied to a particular product synthesis may not be able to describe the phenomenon of interest for other products. As they specifically represent the particular system, they cannot address the kinetics of esterase production. Hence, the aim of this present work is to develop an unstructured model for esterase production by *Saccharomyces cerevisiae*. Unstructured kinetic models are the simplest ones for modeling microbial systems. This modeling strategy describes the microorganisms as an abstract sense, called biomass. Biomass is considered to be a component or reactant in the system. Unstructured kinetic models are the most frequently employed for modeling microbial systems because of their simplicity and are good enough for technical purposes [7, 27]. Because unstructured models are simpler than the structured models, they require the measurement of a smaller number of components and yet are able to describe the evolution of biomass, substrate consumption, and production formation [1, 2]. Mathematical models of fermentation

**Corresponding author*
Phone: 91-9840708563; Fax: 91-44-22574152;
E-mail: pandaiitm@yahoo.co.in

kinetics facilitate data analysis and may provide a strategy for solving problems encountered in industrial fermentation processes [15, 25, 30].

Materials and Methods

Microorganism

Saccharomyces cerevisiae MTCC 36 was obtained from the Microbial Type Culture Collection, Institute of Microbial Technology, Chandigarh, India. The organism was maintained on yeast extract-peptone-dextrose-malt extract-agar slants containing (g/l): yeast extract, 3; peptone, 5; dextrose, 10; malt extract, 3; agar, 20. Slants were incubated at 30°C for 48 h for proper growth. The composition of production media for esterase production was optimized using central composite design (g/l): yeast extract, 2.926; peptone, 7.109; dextrose, 13.765; malt extract, 3.028 [19].

Experimental Method

The 150 ml of medium was placed in a 500-ml Erlenmeyer flask. After sterilization of the medium, approximately 1×10^8 cells were inoculated into the medium. The culture was incubated on a rotary shaker maintained at 180 rpm at 30°C. Samples were collected at regular intervals and were analyzed for glucose, enzyme, and cell mass. Glucose was estimated by the dinitrosalicyclic acid method [17]. Cell mass was measured by the method suggested by Panda and Gowrishankar [19]. An aliquot of 1 ml of sample from fermentation broth was centrifuged at 4,000 rpm for 10 min. After centrifugation, the supernatant was decanted and again centrifuged with water for washing the cells. Cells were then transferred to a preweighted aluminum foil and kept in a drier at 60°C for 12 h or to a time until constant weight was reached. After drying, the weight of the aluminum foil with cells was measured. The amount of cell mass was calculated from the difference between the weight of foil with cells to the weight of the empty foil.

Enzyme Assay

Esterase was assayed by using *p*-nitrophenylacetate as the substrate. A reaction mixture containing 0.5 ml of enzyme solution, 1 ml of 0.15 M sodium phosphate buffer (pH 7.0), 2.5 ml of double-distilled water, and 1 ml of 1 mM substrate solution was incubated at 30°C for 30 min. A standard plot of *p*-nitrophenol *vs.* absorbance at 400 nm was used to find the concentration of liberated *p*-nitrophenol in the reaction mixture [28]. The enzyme activity was expressed in terms of Unit (U). One unit of esterase activity is defined as the amount of enzyme producing 1 μmole of the *p*-nitrophenol per minute under the standard assay conditions. Specific esterase activity is defined as the unit of esterase activity (U) per gram of dry cell mass equivalent (*i.e.*, U/g dry cell mass).

Theory

The mathematical model consists of a set of ordinary differential equations taking into account the microbial growth, the substrate consumption, and the product formation with time. In the logistic model, the rate of cell mass increase may be limited by cell density [5]. Parameter X_m is the upper limit of cell growth and it is called carrying capacity. If cell mass exceeds X_m, the cell growth rate becomes negative and cell numbers decline. The model is based on several assumptions. The specific growth rate depends on substrate concentration. Autoinhibition is assumed to occur within the cell itself. Substrate consumption is not related to the product formation (*i.e.*, intracellular enzyme) and the product formation rate can be associated with the growth of cells. The rates are given below:

$$\frac{dX}{dt}=\frac{\mu_m S}{K_s+S}X\left[1-\frac{X}{X_m}\right] \tag{1}$$

$$\frac{dS}{dt}=-\frac{1}{Y_{X/S}}\frac{dX}{dt} \tag{2}$$

$$\frac{dP}{dt}=Y_{P/X}\frac{dX}{dt} \tag{3}$$

The expression $(1-X/X_m)$ is employed in cell growth rate to describe the autoinhibition of the cell itself [31]. The parameters needed to be evaluated from the model using experimental data are the maximum specific growth rate (μ_m), Monod's constant (K_s), maximum cell mass (X_m), the yield coefficient of cell with respect to substrate ($Y_{x/s}$), and the yield coefficient of product with respect to cell ($Y_{p/x}$).

The model is supplemented with the data of three independent runs. The ordinary differential Eqs. (1)–(3) are solved simultaneously by using the fourth-order Runge-Kutta method, coupled with the optimization procedure called simulated annealing. The initial conditions for solving the ordinary differential equations are $X_0=0.1$ g/l, $P_0=0$, and substrate concentration differs for various concentrations of glucose. The algorithm for parameter estimation procedure is given in Appendix I. The objective function is to minimize the sum of the errors between experimental data and estimated values at all times. The parameters varied one at a time randomly to get a new set of parameters for the algorithm. With each set of parameters, the objective function is determined and the difference in the objective function (Δf) with old and new sets of parameters is calculated. If the new set of values improves the objective function, the move is accepted. Otherwise, the move is accepted with a probability of $\exp(-\Delta f/T)$, where T is simulated annealing temperature, a dummy variable that is used to control the acceptance of uphill moves. Initially, T is fixed at a higher value and is periodically annealed by proportional cooling schedule in the outer loop. At any specific temperature, the parameters are randomly varied number of times in the inner loop. Thus, the optimum parameter values are obtained after T reaches a desired lower value [14]. The algorithm for simulated annealing procedure is given in Appendix II.

Parameter Sensitivity Analysis

The aim of the sensitivity analysis is to estimate a rate of change in the output of the model with respect to changes in model input. This is important for evaluating the applicability of the model, determining parameters, which is important to have more accurate results, and understanding the behavior of the system being modeled. The normalized sensitivity coefficients represent a percentage change in the predicted values due to a percentage change in the parameter values [22].

Results and Discussion

Discussion on Experimental Results

To develop a suitable model, it is necessary that the model should be tested with experimental results. In this regard,

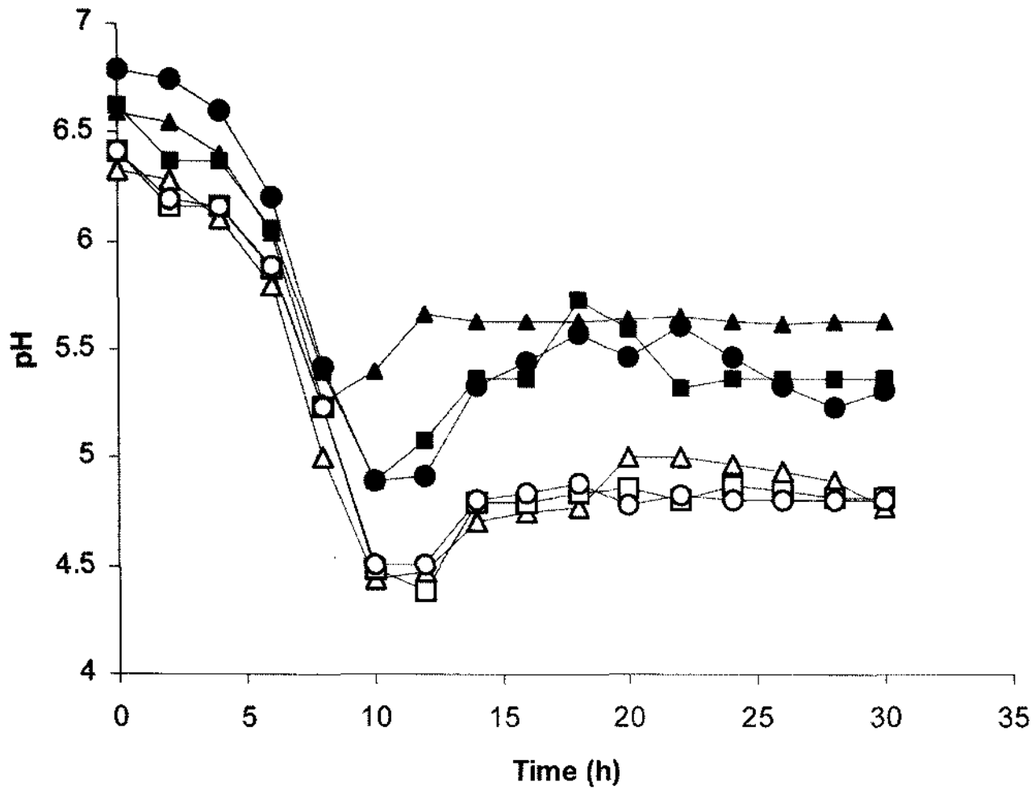

Fig. 1. pH of the medium versus time for different glucose concentrations during fermentation.
For initial glucose concentration: (▲) 4 g/l; (■) 8 g/l; (●) 13.5 g/l; (△) 20 g/l; (□) 22 g/l; (○) 25 g/l.

basic data of cell mass, product concentration, and reactant concentration must be available under a variety of conditions. Current work focused on the fundamental requirement of experimental data for a complex biological reaction. As the fermentation progressed, the pH of the medium decreased exponentially up to 10 h and then remained constant (Fig. 1). The decrease of pH with time may be due to the degradation of glucose yielding acid products in the broth. In this work, the pH of the medium for esterase production was uncontrolled (pH was 6.5). The optimum pH reported for esterase production from *S. cerevisiae* is 6.2 [19]. It may be inferred from Fig. 2 that the glucose consumption with time is analogous to the pH profile. As the glucose concentration decreased with time, the pH of the production medium also decreased with time. For 4 g/l of glucose, some residual glucose was present, whereas for higher concentrations of glucose, the residual glucose in the bulk medium was approximately zero at 20 h of fermentation. On the other hand, microorganism took the same time to attain a plateau irrespective of the glucose concentration. For various glucose concentrations, the lag phase was almost the same (*i.e.*, 2 h), and the stationary phase started approximately at 20 h. Between 2 and 20 h, cells grew exponentially and the amount of cell produced depended on the initial glucose concentration. For low substrate concentration, the amount of dried cell mass per liter of fermentation broth was low and it increased for higher glucose concentrations up to 13.5 g/l. Above 13.5 g/l of glucose, there was no difference in cell mass. The cell growth profiles for 13.5 g/l, 20 g/l, 22 g/l, and 25 g/l of glucose concentrations appeared to be the same between 15 and 20 h. Therefore, the addition of more glucose beyond 13.5 g/l does not influence the cell growth. The maximum dry cell mass obtained at 13.5 g/l is approximately 8.5 g/l (Fig. 3). The products of the fermentation process are proteins. The protein extract obtained after cell lyses, contains more number of proteins. The activity of esterase was measured for different glucose concentrations (Fig. 4). Since esterase is an intracellular protein, the esterase activity profile is similar to the cell mass profile. Even though the amount of dry cell mass for 13.5 g/l and 20 g/l was the same, the esterase activity was high for 20 g/l compared with 13.5 g/l of glucose concentration. The excess glucose present in 20 g/l may be consumed for the synthesis of enzymes rather than the multiplication of cells. Esterase

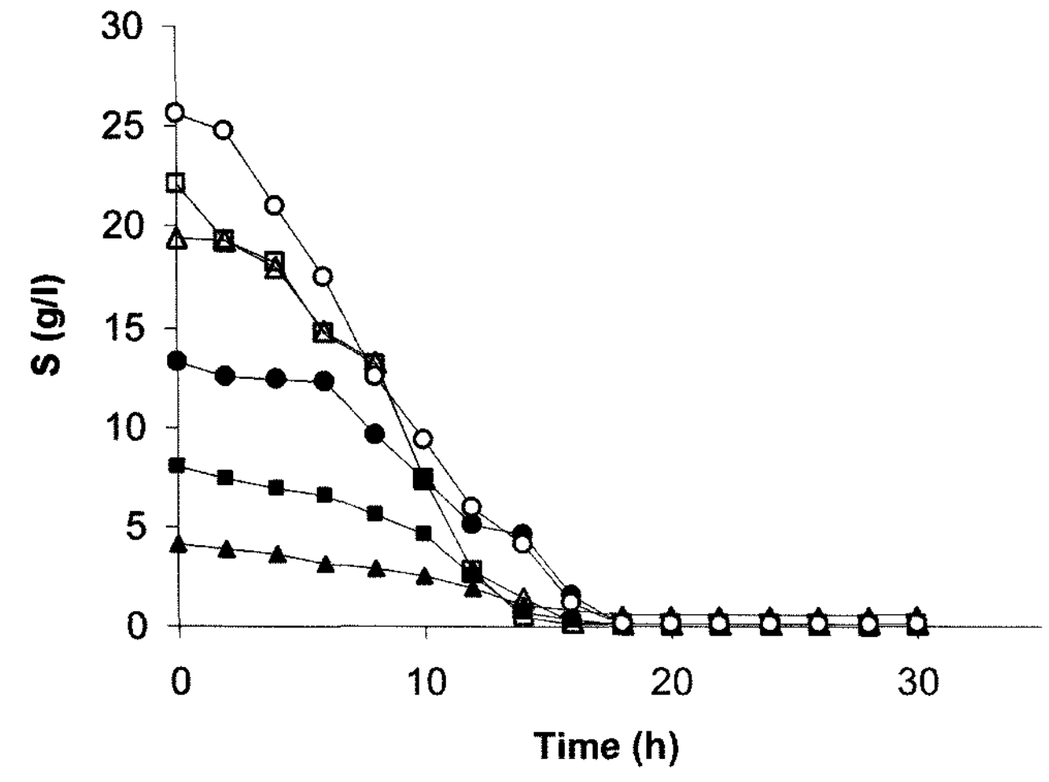

Fig. 2. Glucose concentration versus time for different initial concentrations.
For initial glucose concentration: (▲) 4 g/l; (■) 8 g/l; (●) 13.5 g/l; (△) 20 g/l; (□) 22 g/l; (○) 25 g/l.

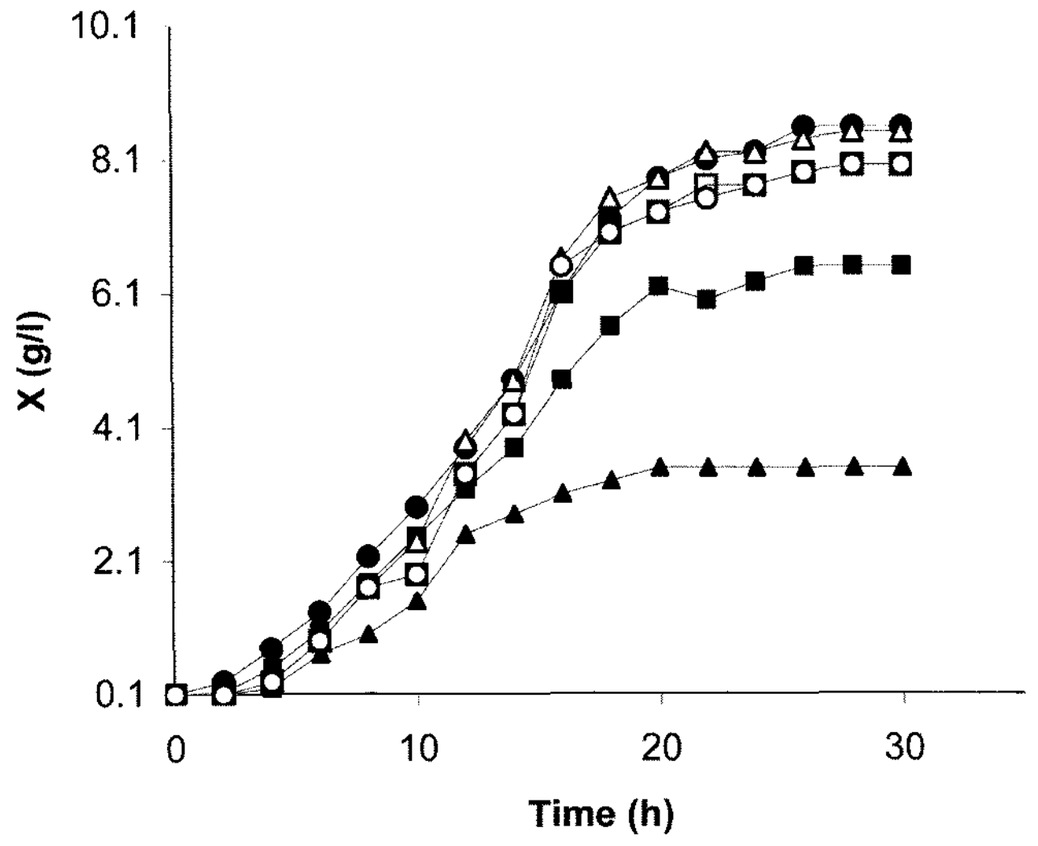

Fig. 3. Cell mass versus time for different glucose concentrations.
For initial glucose concentration: (▲) 4 g/l; (■) 8 g/l; (●) 13.5 g/l; (△) 20 g/l; (□) 22 g/l; (○) 25 g/l.

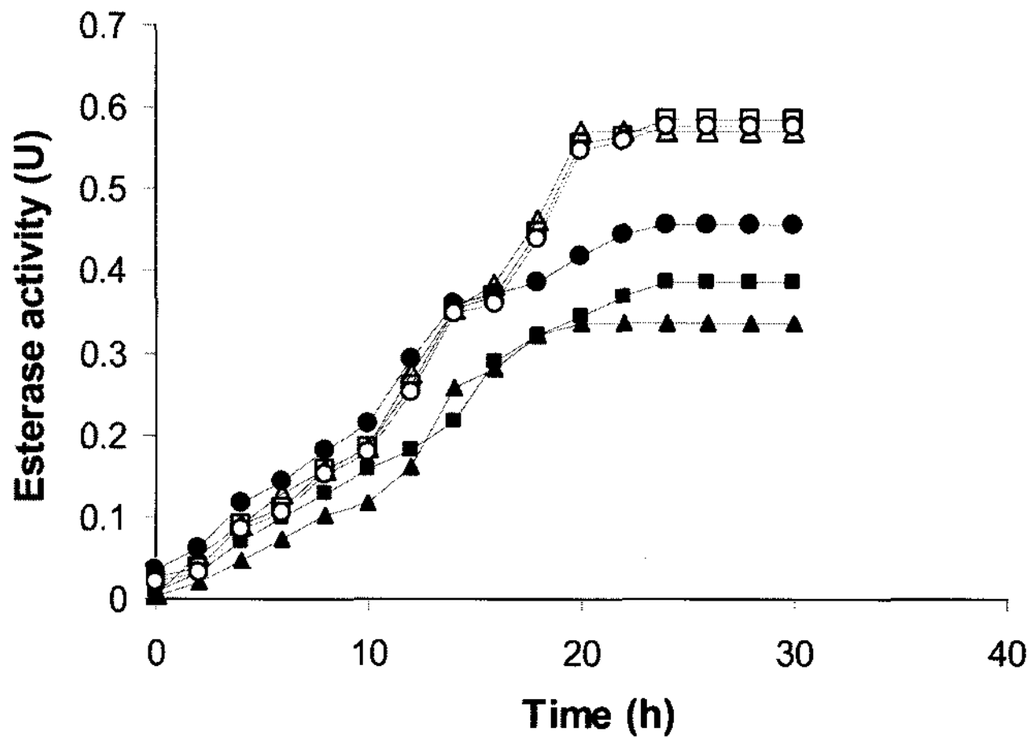

Fig. 4. Esterase activity versus time for different glucose concentrations.
For initial glucose concentration: (▲) 4 g/l; (■) 8 g/l; (●) 13.5 g/l; (△) 20 g/l; (□) 22 g/l; (○) 25 g/l.

activity increased with the increase in initial glucose concentration in the fermentation medium.

Discussion on Theoretical Results

Usually, the cell growth rate is expressed in terms of Monod's equation. In this work, a logistic model has been used to predict the cell growth rate more accurately than the Monod's equation. Fig. 5 shows the difference between the logistic model and Monod's equation for cell mass, glucose concentration, and esterase activity. This shows that the logistic model, having an autoinhibition term in the expression, fits with experimental data very well compared with the Monod's equation. As the intracellular enzymes are associated only with the cells, the substrate consumption is related to the growth of the cells alone. The expression of product formation assumes that the rate of product formation is associated with the cell growth [6]. The experimental data for esterase activity is not able to fit well with the Luedeking-Piret equation because the Luedeking-Piret expression contains both growth-associated and nongrowth-associated terms.

The comparison of experimental data with model curves for cell growth, glucose consumption, and esterase activity at different glucose concentrations are given in Figs. 6–8. The differential Eqs. (1)–(3) are simultaneously solved using the Runge-Kutta method in the MATLAB environment, as discussed in Appendix I. The errors of data for cell growth, glucose consumption, and esterase activity have been calculated individually, plus the total error, which is the sum of all the three individual errors, is minimized by generating new parameter values by the simulated annealing procedure (*cf.* Appendix II).

Fig. 6 shows that Eq. (1) is able to predict well the cell mass data. The correlation coefficients between the

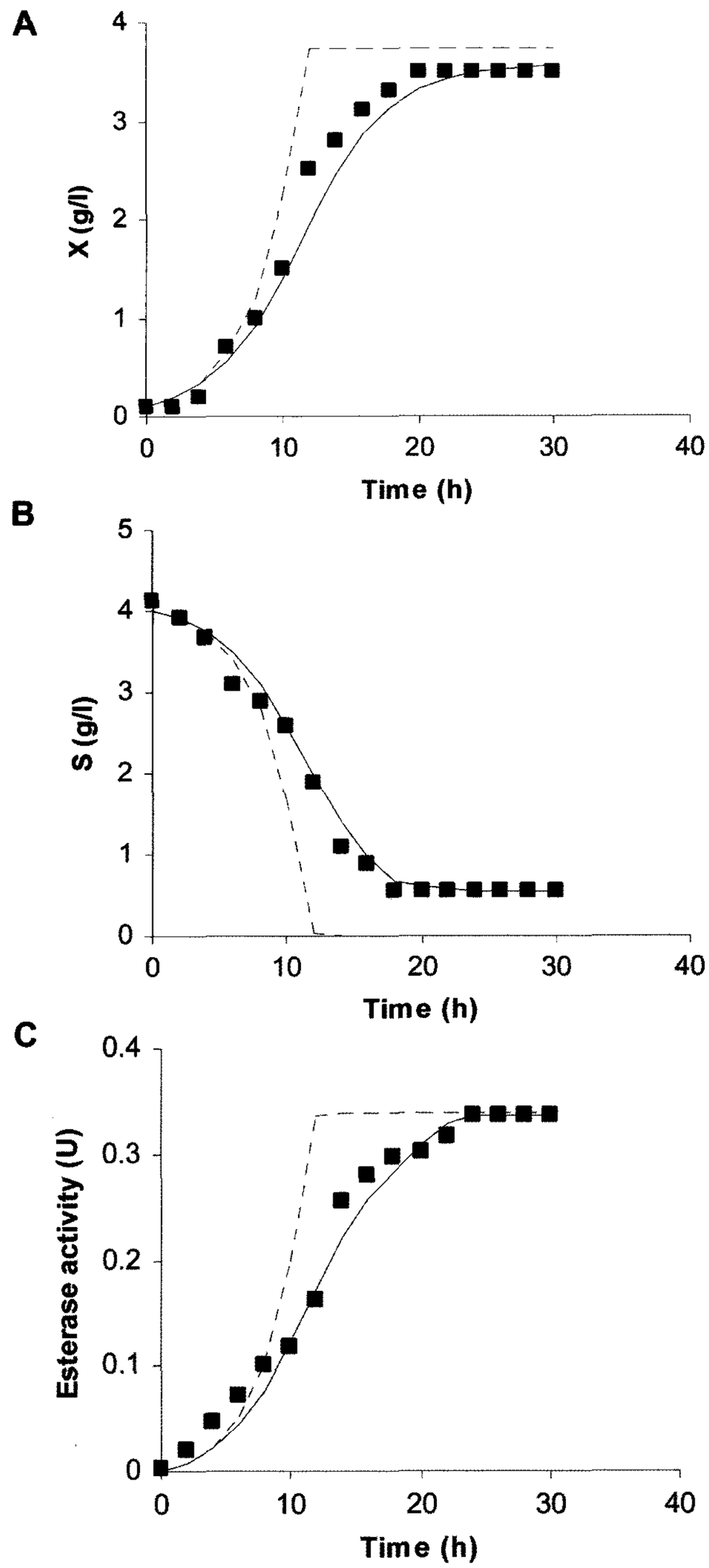

Fig. 5. Comparison between the Monod's equation and the logistic model for 4 g/l of initial glucose concentration: **A** cell mass; **B** glucose concentration; **C** esterase activity.
(■) Experimental data, (—) logistic model, (----) Monod equation.

experimental data and model curves are given in Table 1. The correlation coefficient value implies that the predicted data fits well with the experimental data. Figs. 6–8 show that at low concentrations of glucose in fermentation, the prediction is better compared with the high glucose concentration in the medium. The accuracy of the model was tested using the Student's *t*-test. There was no

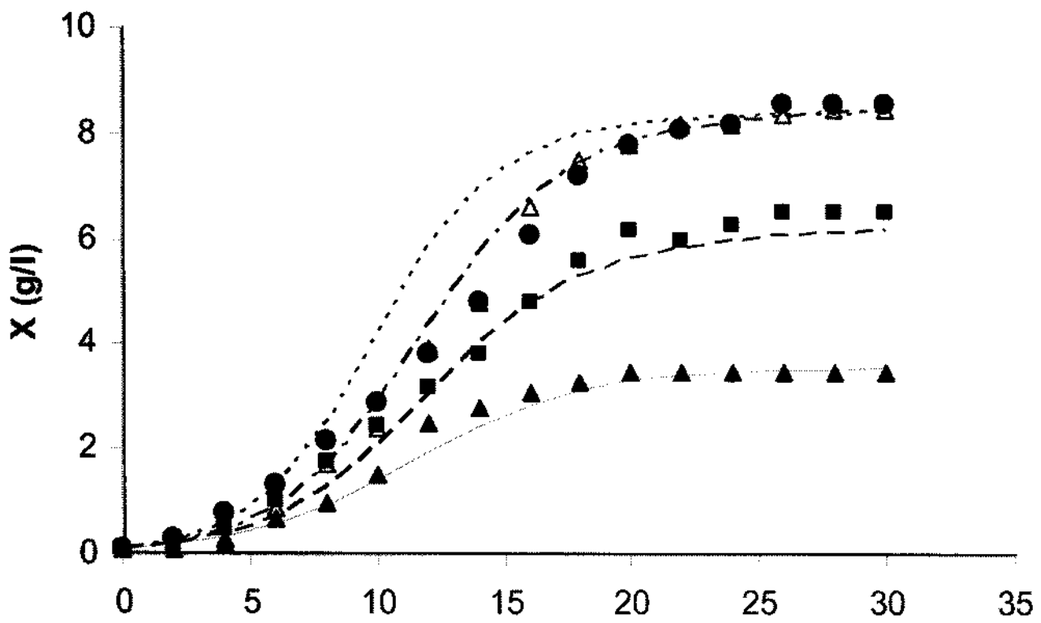

Fig. 6. Comparison of experimental data with model curves for cell mass obtained for different glucose concentrations.
For initial glucose concentration: 4 g/l - (▲) experimental, (——) predicted; 8 g/l - (■) experimental, (- - -) predicted; 13.5 g/l - (●) experimental, (·····) predicted; 20 g/l - (△) experimental, (·····) predicted.

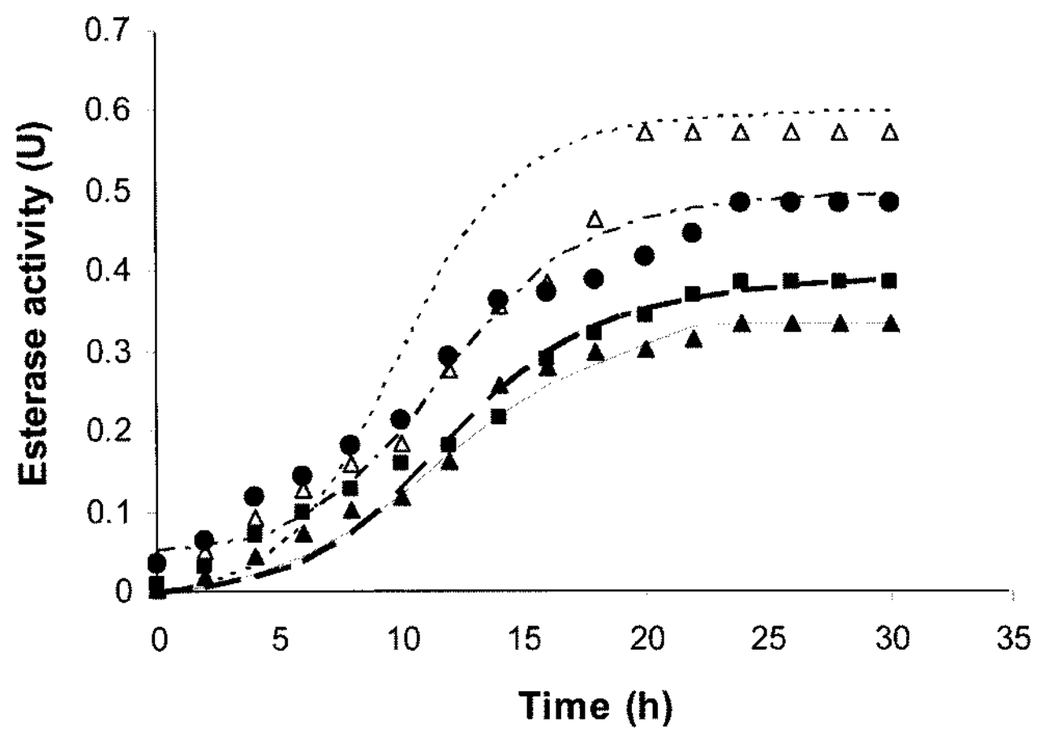

Fig. 8. Comparison of experimental data with model curves for esterase activity obtained for different glucose concentrations.
For initial glucose concentration: 4 g/l - (▲) experimental, (——) predicted; 8 g/l - (■) experimental, (- - -) predicted; 13.5 g/l - (●) experimental, (·····) predicted; 20 g/l - (△) experimental, (·····) predicted.

significant difference observed between the experimental and the estimated data.

The optimum values of the parameters are given in Table 2 for different initial glucose concentrations in the fermentation. It was observed that yield coefficient $Y_{x/s}$ decreased with increasing initial glucose concentration. The maximum amount of dry cell mass (X_m) obtained from the model was approximately the same as that obtained from the experimental data. The main advantage of this logistic model is to predict the maximum amount of dry cell mass at a known initial glucose concentration [16].

Parameter sensitivity analysis has been done by changing the parameter value by 10% of the optimal value. This analysis has been studied by changing only one parameter at a time, keeping other parameters at the optimum value. The variation of sensitivity coefficient with time for the prediction of cell mass, glucose consumption, and esterase activity is given in Fig. 9. It is known that the parameters (μ_m, K_s, X_m, $Y_{x/s}$, and $Y_{p/x}$) are constants for a particular organism and also for the particular conditions. The goal of this sensitivity analysis study is to highlight the importance of the optimum value of the parameter and to analyze the deviation in prediction by changing the parameter values.

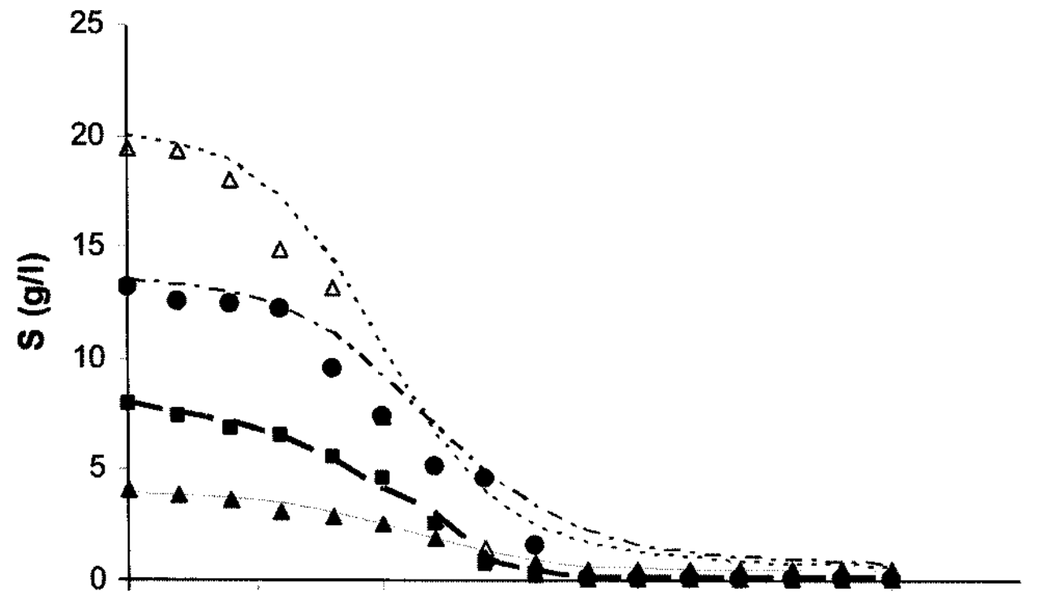

Fig. 7. Comparison of experimental data with model curves for different glucose concentrations.
For initial glucose concentration: 4 g/l - (▲) experimental, (——) predicted; 8 g/l - (■) experimental, (- - -) predicted; 13.5 g/l - (●) experimental, (·····) predicted; 20 g/l - (△) experimental, (·····) predicted.

Table 1. Correlation coefficient between the predicted and experimental data for various glucose concentrations.

Glucose concentration (g/l)	Correlation coefficient for varying X, S, and P		
	For X	For S	For P
4	0.9932	0.9913	0.9883
8	0.9899	0.9607	0.9807
13.5	0.9865	0.9867	0.9878
20	0.9503	0.9836	0.9227
22	0.9545	0.9597	0.9265
25	0.9521	0.9658	0.9234

Table 2. Optimum values of parameters for various glucose concentrations.

Glucose concentration (g/l)	μ_m (1/h)	K_s (g/l)	X_m (g/l)	$Y_{x/s}$* (g/g)	$Y_{p/x}$* (U·l/g)
4	0.3217	0.1145	3.5980	0.9116	0.0930
8	0.3924	1.0991	6.5058	0.7778	0.0638
13.5	0.4124	1.1876	8.5650	0.6558	0.0532
20	0.4755	1.2655	8.4624	0.4310	0.0725
22	0.4732	1.2749	8.5130	0.3419	0.0733
25	0.4779	1.2905	8.5090	0.3102	0.0714

*Evaluated at X_m.

The change in maximum specific growth rate value greatly influences the predicted values of all variables. The predicted value of maximum specific growth rate deviated by more than 20% from the original value for cell mass and esterase activity. K_s and X_m did not influence much on any variables. $Y_{x/s}$ showed similar behavior as did maximum specific growth rate. The variation in $Y_{p/x}$ can only change the esterase activity profile. The study of parameter analysis shows that the predicted values of esterase activity were affected by changing any of the parameter values. $Y_{p/x}$ had no influence on substrate consumption. The prediction of cell concentration values was also not affected by the change in $Y_{p/x}$.

The logistic model was able to predict the esterase activity displayed by *Saccharomyces cerevisiae*. It was found that 20 g/l of glucose concentration produced the maximum esterase activity. Parameter sensitivity analysis showed that even a 10% change in the optimum values has more influence in changing the predicted values. Although the logistic model could estimate the output approximately similar to the experimental data, it is inefficient in describing the mechanism of producing the esterases. More detail about the kinetics of esterase production can be obtained by considering the metabolic pathway using a structured model.

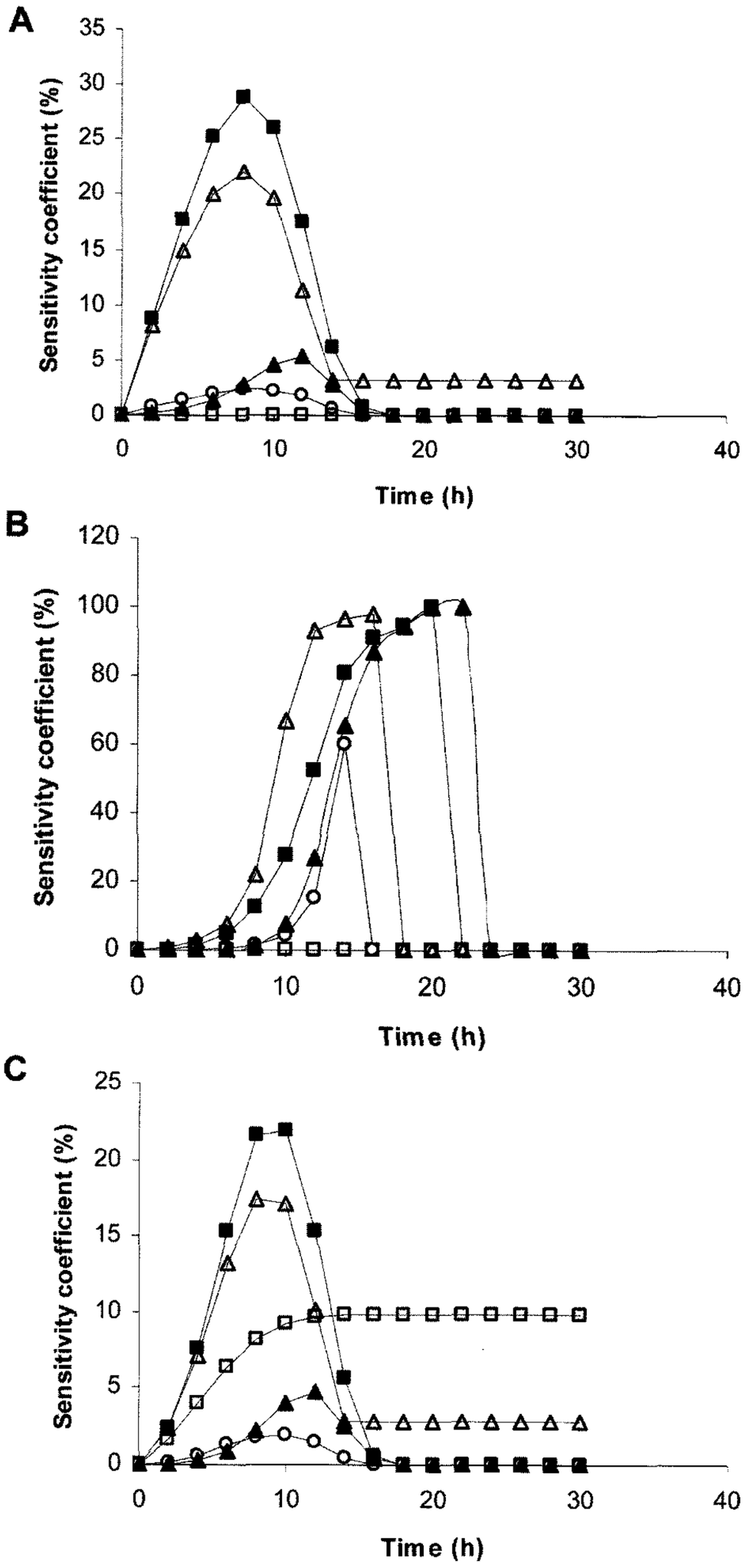

Fig. 9. Sensitivity coefficients versus time for the five parameters: (**A**) variation with cell mass; (**B**) variation with glucose consumption; (**C**) variation with esterase activity.
(■) μ_m; (○) K_s; (▲) X_m; (△) $Y_{x/s}$; (□) $Y_{p/x}$.

NOMENCLATURE

K_s - Monod's constant (g/l)
P - Esterase activity (U)
S - Substrate (or) glucose concentration (g/l)
t - Time (h)
X - Cell concentration (g/l)
X_m - Maximum cell concentration (g/l)
$Y_{p/x}$ - Yield coefficient (U·l/g)
$Y_{x/s}$ - Yield coefficient (g/g)
μ_m - Maximum specific growth rate (1/h)
Δf - Objective function

REFERENCES

1. Amrane, A. and Y. Prigent. 1999. Analysis of growth and production coupling for batch cultures of *Lactobacillus helveticus* with the help of an unstructured model. *Process Biochem.* **34:** 1–10.
2. Burhan, N., Ts. Sapundzhiev, and V. Beschkov. 2005. Mathematical modeling of cyclodextrin-glucanotransferase production by batch cultivation. *Biochem. Eng. J.* **24:** 73–77.
3. Chung, K.-H., J.-S. Park, H.-S. Hwang, J.-C. Kim, and K.-Y. Lee. 2007. Detection and kinetics of mucosal pathogenic bacteria binding with polysaccharides. *J. Microbiol. Biotechnol.* **17:** 1191–1197.
4. El Enshasy, H., Y. A. Fattah, A. Atta, M. Anwar, H. Omar, S. Abou El Magd, and R. Abou Zahra. 2008. Kinetics of cell growth and cyclosporin A production by *Tolypocaldium inflatum* when scaling up from shake flask to bioreactor. *J. Microbiol. Biotechnol.* **18:** 128–134.
5. Gabriel, J.-P., S. Francis, and L. F. Bersier. 2005. Paradoxes in the logistic equation? *Ecol. Modeling* **185:** 147–151.
6. Garcia-Ochoa, F. and J. A. Casas. 1999. Unstructured kinetic model for sophorolipid production by *Candida bombicola*. *Enzyme Microb. Technol.* **25:** 613–621.
7. Garcia-Ochoa, F., V. E. Santos, and A. Alcón. 1998. Metabolic structured kinetic model for xanthan production. *Enzyme Microb. Technol.* **23:** 75–82.

8. Gil, K.-I. and E. S. Choi. 2002. Estimation of nitrite concentration in the biological nitration process using enzymatic inhibition kinetics. *J. Microbiol. Biotechnol.* **12:** 377–381.
9. Hatzakis, N. S., D. Daphnomili, and I. Smonou. 2003. Ferulic acid esterase from *Humicola insolens* catalyzes enantioselective transesterification of secondary alcohols. *J. Mol. Catal. B Enzymatic* **21:** 309–311.
10. Heinzle, E. and R. M. Lafferty. 1980. A kinetic model for growth and synthesis of poly-β-hydroxybutyric acid (PHB) in *Alcaligenes eutrophus* H 16. *Eur. J. Appl. Microbiol. Biotechnol.* **11:** 8–16.
11. Huang, C.-J. and C.-Y. Chen. 2006. Functions of the C-terminal region of chitinase ChiCW from *Bacillus cereus* 28-9 in substrate-binding and hydrolysis of chitin. *J. Microbiol. Biotechnol.* **16:** 1897–1903.
12. Jaeger, K. E., T. Eggert, A. Eipper, and M. T. Reetz. 2001. Directed evolution and the creation of enantioselective biocatalysts. *Appl. Microbiol. Biotechnol.* **55:** 519–530.
13. Kim, J.-N., M.-J. Seo, E.-A. Cho, S.-J. Lee, S.-B. Kim, C.-I. Cheigh, and Y.-R. Pyun. 2005. Screening and characterization of an esterase from a metagenomic library. *J. Microbiol. Biotechnol.* **15:** 1067–1072.
14. Kirkpatrick, S. 1984. Optimization by simulated annealing: Quantitative studies. *J. Stat. Phys.* **34:** 975–986.
15. Kwon, C. H., D. Y. Shin, J. H. Lee, S. W. Kim, and J. W. Kang. 2007. Molecular modeling and its experimental verification for the catalytic mechanism of *Candida antarctica* lipase B. *J. Microbiol. Biotechnol.* **17:** 1098–1105.
16. Mirón, J., M. P. González, L. Pastrana, and M. A. Murado. 2002. Diauxic production of glucose oxidase by *Aspergillus niger* in submerged culture. A dynamic model. *Enzyme Microb. Technol.* **31:** 615–620.
17. Miller, G. L. 1959. Use of dinitrosalicyclic acid reagent for determination of reducing sugar. *Anal. Chem.* **31:** 426–428.
18. Panda, T. and B. S. Gowrishankar. 2005. Production and applications of esterases. *Appl. Microbiol. Biotechnol.* **67:** 160–169.
19. Panda, T. and B. S. Gowrishankar. 2007. Critical analysis of application of generalized distence function for optimization of important variables for eaterase synthesis by *Saccharomyces cerevisiae*. *Biores. Technol.* (in Press).
20. Park, H.-J., Y.-J. Kim, and H.-K. Kim. 2006. Expression and characterization of a new esterase cloned directly from *Agrobacterium tumefaciens* genome. *J. Microbiol. Biotechnol.* **16:** 145–148.
21. Park, K.-M., M. W. Song, S.-J. Kang, and J.-H. Lee. 2007. Batch and continuous culture kinetics for production of carotenoids by β-ionone-resistant mutant of *Xanthophyllomyces dendrorhous*. *J. Microbiol. Biotechnol.* **17:** 1221–1225.
22. Paul, G. C. and C. R. Thomas. 1996. A structured model for hyphal differentiation and penicillin production using *Penicillium chrysogenum*. *Biotechnol. Bioeng.* **51:** 558–572.
23. Rosen, T. C. and T. Daubmann. 2005. Esterases - industrial biocatalysts for mild and selective hydrolysis reactions. *Chem. Today* **23:** 36–38.
24. Sathyanarayana, G. N. and T. Panda. 2003. Analysis of kinetic data of pectinases with substrate inhibition. *J. Microbiol. Biotechnol.* **13:** 332–337.
25. Seo, K.-Y., S.-K. Heo, C. Lee, D. H. Chung, M.-G. Kim, K.-H. Lee, K.-S. Kim, G.-J. Bahk, D.-H. Bae, K.-Y. Kim, C.-H. Kim, and S.-D. Ha. 2007. Development of predictive mathematical model for the growth kinetics of *Staphylococcus aureus* by response surface model. *J. Microbiol. Biotechnol.* **17:** 1437–1444.
26. Sousa, H. A., C. A. M. Afonso, J. P. B. Mota, and J. G. Crespo. 2003. Enantioselective hydrolysis of a *meso*-diester using pig liver esterase in a two-phase stirred tank reactor. *Ind. Eng. Chem. Res.* **42:** 5516–5525.
27. Thilakavathi, M., T. Basak, and T. Panda. 2007. Modeling of enzyme production kinetics. *Appl. Microbiol. Biotechnol.* **73:** 991–1007.
28. Toshimitsu, N., H. Hamada, and M. Kojima. 1986. Purification and some properties of an esterase from yeast. *J. Ferment. Technol.* **64:** 459–462.
29. Venkatesh, K. V., M. R. Okos, and P. C. Wankat. 1993. Kinetic model of growth and lactic acid production from lactose by *Lactobacillus bulgaricus*. *Process Biochem.* **28:** 231–241.
30. Weiss, R. M. and D. F. Ollis. 1980. Extracellular microbial polysaccharides. I. Substrate, biomass, and product kinetic equations for batch xanthan gum fermentation. *Biotechnol. Bioeng.* **22:** 859–873.
31. Zhang, X. W., X.-D. Gong, and F. Chen. 1999. Kinetic models for astaxanthin production by high cell density mixotrophic culture of the microalga *Haematococcus pluvialis*. *J. Ind. Microbiol. Biotechnol.* **23:** 691–696.

APPENDIX I

Parameter Estimation Method

Ordinary differential equations are solved by using Runge-Kutta method. The syntax used is as follows,

```
[t , c]=ode45(F, [t0, tf], c0)
```

where, t0=initial time
tf=final time
c0=vector consists of the initial values of cell concentration, glucose concentration and enzyme activity

Initial concentration considered for solving the model equation are 0.1 g/l and zero for cell mass and esterase activity respectively. The initial concentration for glucose differs for different set of experiments.

Following are the steps involved in solving the differential equations:

- Input the initial guess of parameter values.
- Input the initial conditions of X_0, S_0, P_0.
- Subprogram containing the ordinary differential equations is executed by using the above syntax of Runge-Kutta method.
- Output values obtained are X, S and P with respect to time.

APPENDIX II

Simulated Annealing Algorithm:

- Step 1: The values of **x** and T_{sa} are initialized.
- Step 2: An element of x is choosen randomly and changed it randomly to a new value (*i.e.*, randomly generate $\mathbf{x}^{new}$ in the vicinity of $\mathbf{x}^{old}$).
- Step 3: Objective function is calculated as, $\Delta f=f(\mathbf{x}^{new})-f(\mathbf{x}^{old})$. If $\Delta f<0$ (*i.e.*, if the objective function is improved), then the new vector $\mathbf{x}^{new}$ is accepted. Otherwise, it is accepted with the probability $\exp(-\Delta f/T_{sa})$.
- Step 4: Repeated use of steps 2 and 3, for many times will reduce T_{sa} periodically. The annealing schedule involves reducing the annealing temperature according to the following equation,

$$T_{sa}^{(n+1)}=\xi T_{sa}^{(n)}$$

where ξ is a constant somewhat less than unity and n represents the nth annealing temperature.

as $T_{sa}\rightarrow\infty$, the probability of any move approaches 1

as $T_{sa}\rightarrow 0$, the probability of accepting uphill moves approaches 0.